Acta Crystallographica Section F
Structural Biology and Crystallization Communications
ISSN 1744-3091

Expression, purification and preliminary X-ray crystallographic analysis of cyanobacterial biliverdin reductase

Aya Watanabe,[a] Kunio Hirata,[b] Yoshinori Hagiwara,[a] Yuko Yutani,[a] Masakazu Sugishima,[c] Masaki Yamamoto,[b] Keiichi Fukuyama[a] and Kei Wada[a]*

[a]Department of Biological Sciences, Graduate School of Science, Osaka University, Toyonaka, Osaka 560-0043, Japan, [b]RIKEN SPring-8 Center, Sayo-cho, Hyogo 679-5148, Japan, and [c]Department of Medical Biochemistry, Kurume University School of Medicine, Kurume, Fukuoka 830-0011, Japan

Correspondence e-mail: keiwada@bio.sci.osaka-u.ac.jp

Received 13 October 2010
Accepted 20 December 2010

Biliverdin reductase (BVR) catalyzes the conversion of biliverdin IX α to bilirubin IX α with concomitant oxidation of an NADH or NADPH cofactor. This enzyme also binds DNA and enhances the transcription of specific genes. Recombinant cyanobacterial BVR was overexpressed in *Escherichia coli*, purified and crystallized. A native data set was collected to 2.34 Å resolution on beamline BL38B1 at SPring-8. An SeMet data set was collected from a microcrystal (300 × 10 × 10 µm) on the RIKEN targeted protein beamline BL32XU and diffraction spots were obtained to 3.0 Å resolution. The native BVR crystal belonged to space group $P2_12_12_1$, with unit-cell parameters $a = 58.8$, $b = 88.4$, $c = 132.6$ Å. Assuming that two molecules are present in the asymmetric unit, V_M (the Matthews coefficient) was calculated to be 2.37 Å^3 Da^{-1} and the solvent content was estimated to be 48.1%. The structure of cyanobacterial BVR may provide insights into the mechanisms of its enzymatic and physiological functions.

1. Introduction

Linear tetrapyrrole pigments are widely distributed throughout the kingdoms of life. In phototrophs, linear tetrapyrroles play a central role in both light harvesting and light sensing (Dammeyer & Frankenberg-Dinkel, 2008; Ikeuchi & Ishizuka, 2008). The biosynthesis of linear tetraphyrroles begins with haem degradation (Fig. 1); in phototrophs, the porphyrin ring of haem is cleaved at the *α-meso* carbon bridge by ferredoxin-dependent haem oxygenases to form biliverdin IX α (Frankenberg-Dinkel, 2004; Mantle, 2002), the common precursor of all phytobilins. In cyanobacteria, biliverdin IX α is further reduced to phytobilins by ferredoxin-dependent bilin reductases such as PcyA (Beale, 1993). The biosynthesis of phytobilin from haem has been extensively studied; we have been involved in studying the molecular mechanisms of cyanobacterial haem oxygenase (Sugishima *et al.*, 2004, 2005) and PcyA (Hagiwara *et al.*, 2006, 2010) on the basis of their crystal structures.

In mammals, biliverdin reductase (BVR) catalyzes the reduction of biliverdin IX α using NADH or NADPH to produce the antioxidant bilirubin IX α. Intriguingly, whole-genome analysis revealed that many cyanobacteria possess the *bvr* gene, which encodes the mammalian BVR homologue. *In vitro*, recombinant cyanobacterial BVR converts biliverdin IX α into bilirubin IX α using NADH or NADPH as an electron donor (Schluchter & Glazer, 1997). Disruption of the *bvr* gene in *Synechocytis* sp. PCC6803 perturbs the biosynthesis of phycobiliproteins, which include light-harvesting pigments such as phycocyanobilin. Thus, it has been proposed that the reaction product of cyanobacterial BVR plays a regulatory role in phycobiliprotein biosynthesis (Schluchter & Glazer, 1997), even though bilirubin, which is the product of the *in vitro* BVR reaction, has never been detected in cyanobacterial cells (Ikeuchi & Ishizuka, 2008). Interestingly, mammalian BVR is a serine/threonine kinase that is activated by oxygen radicals and translocates into the nucleus

in response to cGMP and oxidative stress (Maines *et al.*, 2007; Salim *et al.*, 2001). In addition, the dimeric form of human BVR binds to a DNA fragment corresponding to the haem oxygenase 1 promoter region and may play a role in transcriptional activation by oxidative stress (Ahmad *et al.*, 2002). This finding raises the possibility that cyanobacterial BVR also regulates the transcription of the genes involved in phycobiliprotein biosynthesis *in vivo*.

The amino-acid sequences of human (accession No. AAH05902), rat (NP_446302) and cyanobacterial (NP_440117) BVRs share ∼60% similarity over the N-terminal 150 residues. In mammals, BVR contains a leucine zipper-like motif (residues 100–160; Ahmad *et al.*, 2002), a DNA-binding motif that consists of repeats of five residues separated by six amino acids. In contrast, cyanobacterial BVRs do not contain a canonical leucine-zipper motif, although the corresponding region contains periodic leucine residues as well as many basic and hydrophobic residues. Recently, it has been reported that cyanobacterial BVR forms a homodimer (Hayes & Mantle, 2009), which is consistent with the behaviour of a typical DNA-binding protein.

The crystal structures of the apo forms of rat and human BVR and the NAD^+- and $NADP^+$-bound forms of rat BVR have been determined (Kikuchi *et al.*, 2001; Whitby *et al.*, 2002); the configurations of the bound $NAD^+/NADP^+$ and the surrounding residues were also elucidated. The substrate-binding model based on the crystal structure predicted that a conserved Tyr97 in rat BVR might play a central role in the catalytic reaction; however, when this residue was mutated (Y97F) the activity was only reduced by 50% compared with the wild type (Whitby *et al.*, 2002). The identities of both the catalytic residues and the substrate-binding site remain controversial because the binding configuration of the substrate, biliverdin, remains unknown. The DNA-binding site on BVR also remains unknown.

In order to understand the structural basis for DNA binding, as well as biliverdin binding, of cyanobacterial BVR, we initiated the determination of its structure by X-ray crystallographic analysis. In this paper, we describe the overexpression, purification and crystallization of cyanobacterial BVR, as well as our preliminary X-ray diffraction studies.

2. Materials and methods

2.1. Production of native and selenomethionine-substituted BVR

The *slr1784* gene encoding BVR was amplified by PCR from the genomic DNA of *Synechocystis* sp. PCC6803. *Nde*I and *Bam*HI restriction sites (shown in bold) were introduced into the oligonucleotide primers 5′-**CATATG**TCTGAAAATTTTGCAGTTG-3′ and 5′-**GGATCC**GAGCTCAATTTTCAACCTTATATCCACA-3′, respectively. The amplified gene, including the original stop codon, was cloned into pCR2.1-TOPO (Invitrogen) to yield pCR2.1-TOPO/*bvr*. After confirmation of its DNA sequence, pCR2.1-TOPO/*bvr* was digested with *Nde*I and *Bam*HI and cloned into pET21a for nontagged BVR and pET15b (Novagen) for overexpression of the protein with a His_6 tag at its N-terminus.

To overexpress native BVR, *Escherichia coli* strain C41 (DE3) cells (Miroux & Walker, 1996) transformed by heat shock with pET21a/*bvr* were grown at 310 K until the A_{600} reached 0.6 in Terrific Broth containing ampicillin (50 µg ml^{-1}). Overexpression was conducted overnight under shaking at the same temperature after induction by the addition of 1 m*M* IPTG. Cells were harvested by centrifugation at 3000*g* for 30 min. *E. coli* strain B834 (DE3) cells transformed with pET15b/*bvr* were grown at 310 K to overexpress selenomethionine-substituted (SeMet) His_6-BVR. A 20 ml aliquot of a culture grown overnight at 310 K in LB medium was centrifuged at 5000*g* for 1 min and the pellet was then resuspended in 1 ml LeMaster medium and added to 5 l of the same medium containing ampicillin (50 µg ml^{-1}) and selenomethionine (100 µg ml^{-1}). Overexpression was conducted for 48 h at the same temperature after induction by the addition of 1 m*M* IPTG. Cells were harvested by centrifugation at 3000*g* for 30 min.

2.2. Purification

2.2.1. Purification of native BVR. The bacterial pellet (typically 15 g wet weight) was suspended in 40 ml 50 m*M* Tris–HCl pH 7.8 (buffer *A*). Cells were disrupted by sonication and centrifugation

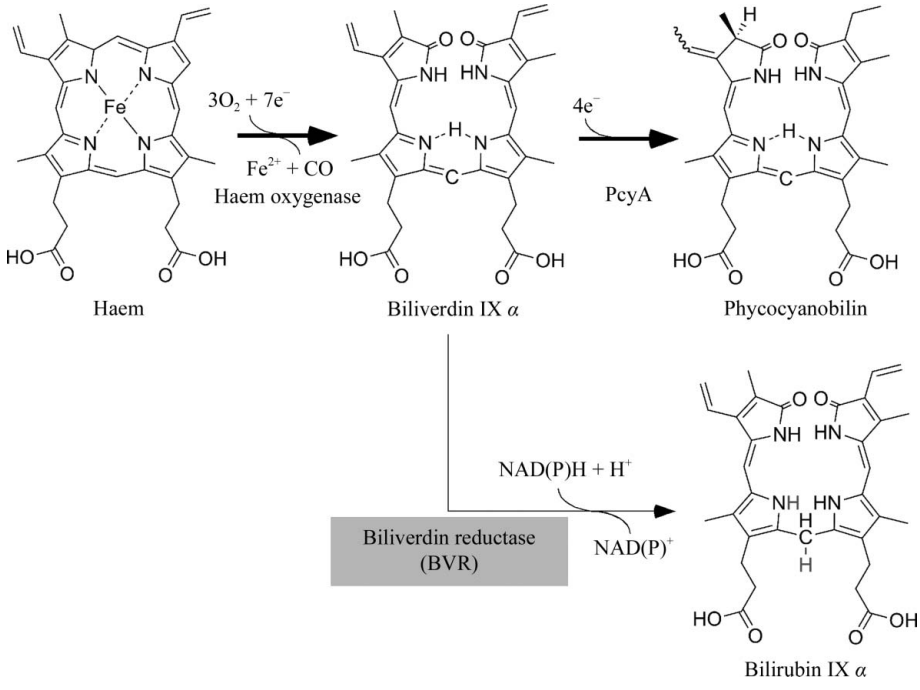

Figure 1
Biosynthesis of linear tetrapyrrole pigments in cyanobacteria (*Synechocystis* sp. PCC 6803).

(8000*g* for 30 min at 277 K). The supernatant containing the soluble native BVR was subjected to ammonium sulfate fractionation at 40% saturation and centrifuged (27 000*g* for 30 min at 277 K). The supernatant was loaded onto a HiPrep 16/10 Butyl FF column (GE Healthcare) equilibrated with 40% ammonium sulfate in buffer *A*. After the column had been washed with buffer *A*, the protein was eluted with a decreasing linear gradient of ammonium sulfate (40–0%). Fractions containing BVR were collected and dialyzed against buffer *A*. The sample was loaded onto a HiLoad 26/10 Q Sepharose HP column (GE Healthcare) equilibrated with buffer *A*. The column was washed with buffer *A* and the protein was eluted with an increasing linear gradient of NaCl (0–500 m*M*). Fractions containing BVR were concentrated using a Vivaspin filter (GE Healthcare) and loaded onto a HiPrep 16/60 Sephacryl S-200 HR gel-filtration column (GE Healthcare) equilibrated with 150 m*M* NaCl in buffer *A*. Fractions containing BVR were monitored by SDS–PAGE analysis. The protein concentration was determined by the Bradford assay using BSA as a reference.

2.2.2. Purification of SeMet BVR. The bacterial pellet (typically 20 g wet weight) was suspended in 40 ml 50 m*M* Tris–HCl pH 7.8, 300 m*M* NaCl and 20 m*M* imidazole (buffer *B*). Cells were disrupted by sonication and centrifugation (8000*g* for 30 min at 277 K). The supernatant containing the soluble His-tagged protein was mixed with His-Accept resin (Nacalai) and incubated for 30 min at 277 K under rotation. The lysate/resin mixture was washed five times with buffer *B*. Protein elution was carried out five times with 50 m*M* Tris–HCl pH 7.8, 300 m*M* NaCl and 300 m*M* imidazole. The eluted fractions were collected and analyzed by SDS–PAGE.

Nontagged SeMet BVR was prepared by digestion of His_6-tagged SeMet BVR with 10 units of thrombin (GE Healthcare) per milligram of protein in PBS buffer (10 m*M* Na_2HPO_4, 1.8 m*M* KH_2PO_4, 2.7 m*M* KCl and 140 m*M* NaCl) pH 7.4 for 48 h at 293 K. The nontagged SeMet BVR was separated from the remaining His-tagged protein by mixing it again with His-Accept resin and incubating for 30 min. The flowthrough fraction containing nontagged SeMet BVR and thrombin was concentrated using a Vivaspin filter and loaded onto a HiPrep 16/60 Sephacryl S-200 HR gel-filtration column (GE Healthcare) equilibrated with PBS buffer.

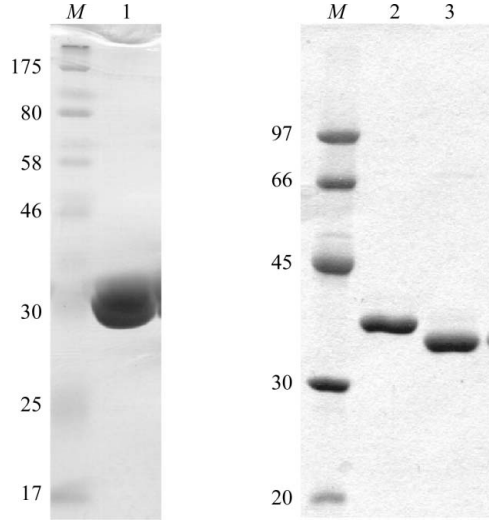

Figure 2
SDS–PAGE analysis of the purified cyanobacterial BVR. Lane *M*, molecular-weight markers (kDa); lane 1, purified native BVR; lane 2, SeMet His_6-BVR; lane 3, purified nontagged SeMet BVR.

2.3. Crystallization

The purified native and SeMet BVR were concentrated using Vivaspin filters. All crystallization trials were carried out using the hanging-drop vapour-diffusion method at 277 K. Crystallization drops consisting of 1 µl protein solution and 1 µl precipitant solution were equilibrated against 200 µl precipitant solution. The initial trials were performed using commercially available sparse-matrix screening kits: Crystal Screen, Crystal Screen 2, Crystal Screen Lite, PEG/Ion and PEG/Ion 2 (Hampton Research), Wizard I–III (Emerald BioStructures) and JB Screen 1–6 (Jena Bioscience GmbH). The initial conditions that produced crystals were optimized by varying the protein concentration, precipitant, buffer system and pH.

2.4. Data collection

The crystals were transferred into a cryoprotectant solution consisting of reservoir solution containing 15%(*v*/*v*) glycerol for a few seconds and then flash-cooled in a cryostream at 100 K. A complete data set for native BVR was collected with an ADSC Quantum 4R detector using synchrotron radiation (λ = 1.000 Å) on SPring-8 beamline BL38B1 (Hyogo, Japan). The crystal-to-detector distance was 200 mm and 180 images were recorded at 1° intervals with an exposure time of 15 s per image. The intensity data were processed and scaled using *HKL*-2000 (Otwinowski & Minor, 1997).

Owing to the small size of the SeMet BVR crystal, data collection was carried out on the RIKEN targeted protein beamline BL32XU at SPring-8, which is dedicated to data collection from protein microcrystals (Hirata *et al.*, 2010). The intensity data set for SeMet BVR was collected with a Rayonix MX225HE CCD detector using a beam size of 1 × 10 µm (horizontal × vertical), a wavelength of 0.9740 Å and a crystal-to-detector distance of 220 mm. After the collection of each two sequential images, the beam-irradiation position was shifted by 1.0 µm with inverse-beam geometry using the SPring-8 data-collection software *BSS* (Ueno *et al.*, 2005). A total of 508 images were collected with an oscillation angle of 1.0°. The intensity data were processed and scaled using *HKL*-2000 (Otwinowski & Minor, 1997).

3. Results

3.1. Purification

When the native form of BVR was overexpressed in *E. coli* strain C41 (DE3), SDS–PAGE of whole cell extracts showed a major Coomassie Blue-stained band at ∼36 kDa, which is consistent with the mass of BVR estimated from its DNA sequence. Purification of the native BVR yielded ∼15 mg protein, the purity of which was evaluated to be greater than 95% using a Coomassie Blue-stained gel (Fig. 2).

We initially attempted to overexpress SeMet BVR in *E. coli* strain B834 (DE3) using pET21a/*bvr*, which encodes nontagged BVR. Because the resulting protein level was very low, we could not obtain purified SeMet BVR in a sufficient quantity for crystallization trials. Hence, we overexpressed SeMet BVR with a histidine tag in B834 (DE3) cells in order to achieve efficient purification. Nickel-affinity purification successfully produced nearly homogeneous SeMet His_6-BVR. The first 17 amino acids from the N-terminus of SeMet His_6-BVR were cleaved with thrombin and subsequent purification steps completely removed the N-terminal His-tag region (Fig. 2). The resulting SeMet BVR contained three additional amino acids (*i.e.*

Gly-Ser-His) at the N-terminus compared with native BVR and three selenomethione residues in each subunit.

3.2. Crystallization

Initial crystallization trials using native BVR produced small crystals in several drops containing polyethylene glycol (PEG) as a precipitant. The crystallization conditions ultimately established consisted of protein at 12 mg ml^{-1} in 50 m*M* Tris–HCl pH 7.8 containing 150 m*M* NaCl and a reservoir solution consisting of 15%(*w*/*w*) PEG 4000, 50 m*M* Tris–HCl pH 7.25, 0.2 *M* sodium acetate and 0.2 m*M* Cymal-2. Crystals grew to maximum dimensions of 0.1 × 0.1 × 0.5 mm (Fig. 3*a*).

Fortunately, microcrystals of nontagged SeMet BVR could be obtained under conditions similar to those that produced the crystals of native BVR. In order to improve the size and shape of the crystals, it was necessary to optimize the crystallization conditions. The best crystals of nontagged SeMet BVR were grown in a drop containing a

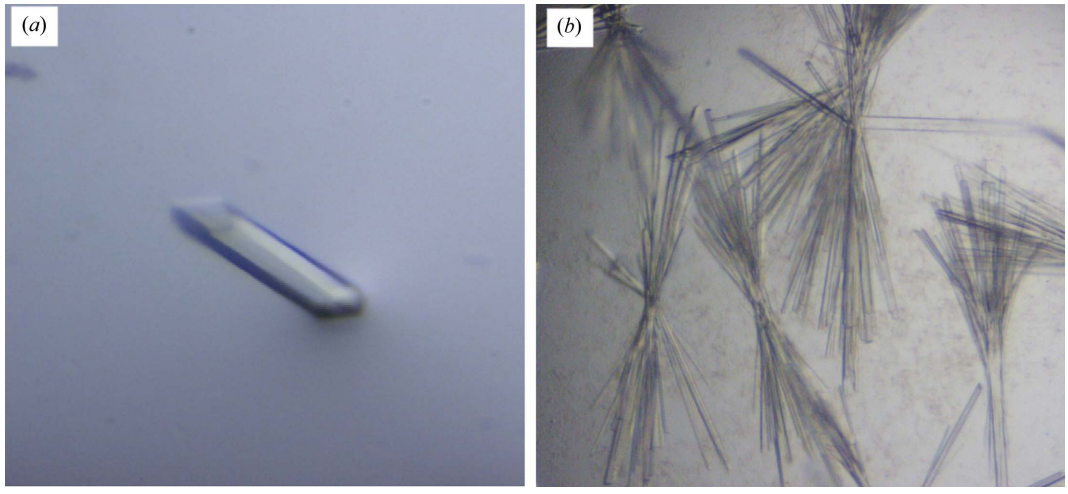

Figure 3
Typical crystals of cyanobacterial BVR. (*a*) Crystals of native BVR. Approximate crystal dimensions are 0.1 × 0.1 × 0.5 mm. (*b*) Microcrystals of nontagged SeMet BVR. Approximate crystal dimensions are 300 × 10 × 10 µm.

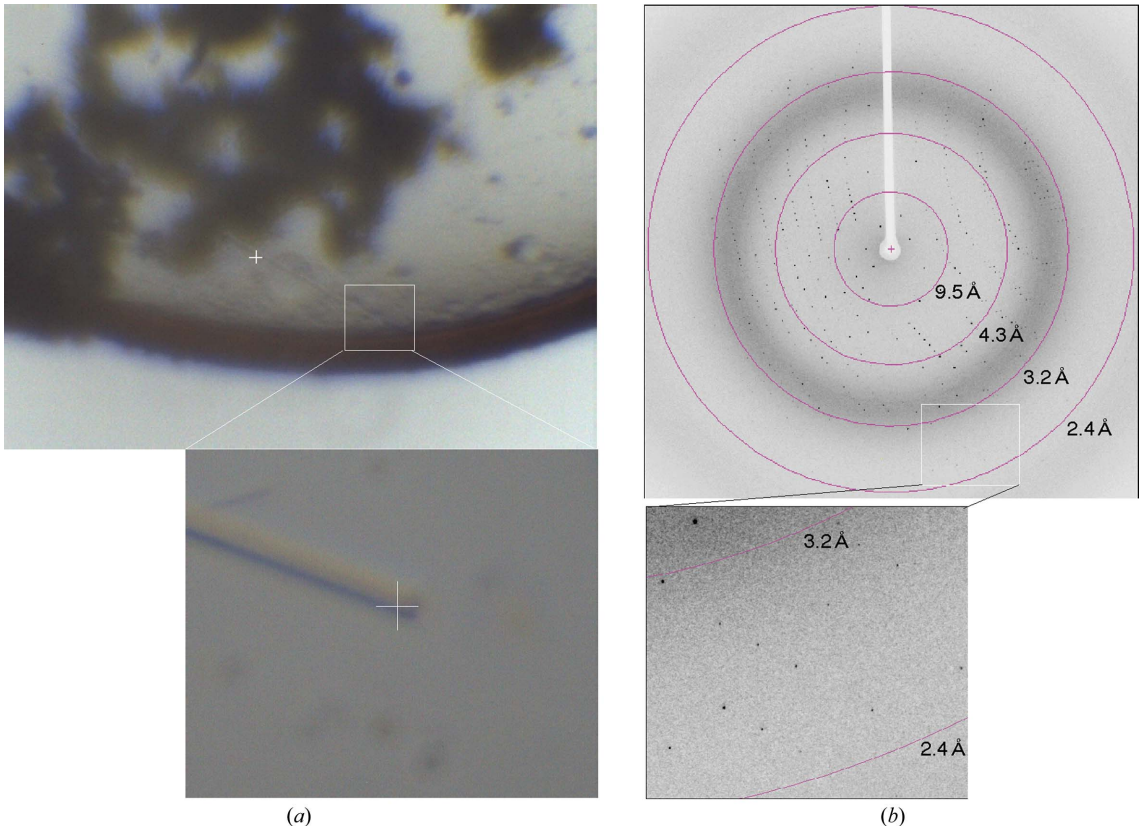

Figure 4
X-ray data collection from SeMet BVR microcrystals. (*a*) A needle-shaped crystal mounted in a loop in a cryogenic stream on SPring-8 beamline BL32XU. Approximate crystal dimensions are 300 × 10 × 10 µm. (*b*) A typical diffraction frame from an SeMet BVR microcrystal.

Table 1
Summary of crystallographic statistics.

Values in parentheses are for the outermost shell.

	Native BVR	SeMet BVR
X-ray source	BL38B1	BL32XU
Wavelength (Å)	1.0000	0.9740
Space group	$P2_12_12_1$	$P2_12_12_1$
Unit-cell parameters (Å)	a = 58.8, b = 88.4, c = 132.6	a = 58.4, b = 87.8, c = 133.7
Resolution range (Å)	50–2.34 (2.42–2.34)	25–3.00 (3.05–3.00)
No. of observations	204988	286322
No. of unique reflections	29740	14380
$R_{\rm merge}$† (%)	5.6 (31.8)	9.8 (31.9)
Multiplicity	6.9 (6.7)	19.9 (20.7)
Completeness (%)	99.9 (99.9)	100.0 (100.0)
Mean $I/\sigma(I)$	11.9 (7.1)	13.6 (3.5)

† $R_{\rm merge} = \sum_{hkl}\sum_i |I_i(hkl) - \langle I(hkl)\rangle| / \sum_{hkl}\sum_i I_i(hkl)$, where $\langle I(hkl)\rangle$ is the mean intensity for multiply recorded reflections.

1:1 mixture of protein solution (12.7 mg ml^{-1} in PBS buffer pH 7.4) and reservoir solution [15%(*w*/*v*) PEG 4000, 0.1 *M* Tris–HCl pH 8.5 and 0.2 *M* sodium acetate]. The crystals grew to maximum dimensions of 300 × 10 × 10 µm in a week (Fig. 3*b*).

3.3. Preliminary X-ray analaysis

An X-ray diffraction experiment using a native BVR crystal was performed on the BL38B1 beamline. The crystal belonged to the orthorhombic space group $P2_12_12_1$, with unit-cell parameters a = 58.8, b = 88.4, c = 132.6 Å. A complete data set was collected to a resolution of 2.34 Å (Table 1). The unit-cell parameters are compatible with the presence of two BVR molecules per asymmetric unit and a solvent content of 48.1% ($V_{\rm M}$ = 2.37 Å^3 Da^{-1}; Matthews, 1968). We attempted to solve the structure of BVR by molecular-replacement methods using apo rat BVR (PDB code 1gcu; 21% sequence identity; Kikuchi *et al.*, 2001), NADH-bound rat BVR (PDB entry 1lc0; 21% sequence identity; Whitby *et al.*, 2002) and human BVR (PDB code 2h63; 21% sequence identity; K. Kavanagh, J. Elkins, E. Ugochukwu, K. Guo, E. Pilka, P. Lukacik, C. Smee, E. Papagrigoriou & U. Oppermann, unpublished work) as search models using the programs *MOLREP* (Vagin & Teplyakov, 1997), *EPMR* (Kissinger *et al.*, 1999) and *MrBUMP* (Keegan & Winn, 2007). Unfortunately, all of the molecular-replacement trials were unsuccessful.

To detect the anomalous signals in the diffraction data, a microcrystal of nontagged SeMet BVR was mounted on beamline BL32XU at SPring-8, where we used a 1 × 10 µm (horizontal × vertical) beam with a photon flux density of 2 × 10^{10} photons s^{-1} µm^{-2}. Irradiation of the single needle-shaped crystal on the loop using a microbeam with exceptionally high brightness permitted diffraction to 3.0 Å resolution (Fig. 4). However, this microbeam caused serious radiation damage to the crystal; the intensities of the reflections in the higher resolution shells decreased rapidly after a couple of frames. We overcame this problem by shifting the beam-irradiation position along the needle axis of the crystal by 1.0 µm after the collection of every two images. This change in irradiation position effectively led to migration of the radiation damage and an intensity data set could be collected from one microcrystal (Table 1). Structure determination is now under way using the SAD and SIRAS methods; we also plan to collect MAD data from the microcrystals.

We thank Drs Seiki Baba, Takeshi Hoshino and Nobuhiro Mizuno (Japan Synchrotron Radiation Research Institute) for their help during data collection with synchrotron radiation at SPring-8 (Hyogo, Japan). The synchrotron-radiation experiments were performed on BL38B1 and BL32XU at SPring-8 with the approval of the Japan Synchrotron Radiation Research Institute (Proposal Nos. 2009A1183, 2009B1219 and 2010B1254). We also thank Professor Yasuhiro Takahashi (Saitama University) for informative discussions and Drs Takakazu Kaneko and Satoshi Tabata (Kazusa DNA Research Institute). This work was partly supported by Grants-in-Aid for Scientific Research to KF (20370037) and KW (21770112) from the Ministry of Education, Culture, Sports, Science and Technology of Japan.

References

Ahmad, Z., Salim, M. & Maines, M. D. (2002). *J. Biol. Chem.* **277**, 9226–9232.
Beale, S. I. (1993). *Chem. Rev.* **93**, 785–802.
Dammeyer, T. & Frankenberg-Dinkel, N. (2008). *Photochem. Photobiol. Sci.* **7**, 1121–1130.
Frankenberg-Dinkel, N. (2004). *Antioxid. Redox Signal.* **6**, 825–834.
Hagiwara, Y., Sugishima, M., Khawn, H., Kinoshita, H., Inomata, K., Shang, L., Lagarias, J. C., Takahashi, Y. & Fukuyama, K. (2010). *J. Biol. Chem.* **285**, 1000–1007.
Hagiwara, Y., Sugishima, M., Takahashi, Y. & Fukuyama, K. (2006). *Proc. Natl Acad. Sci. USA*, **103**, 27–32.
Hayes, J. M. & Mantle, T. J. (2009). *FEBS J.* **276**, 4414–4425.
Hirata, K., Ueno, G., Nisawa, A., Kawano, Y., Hikima, T., Shimizu, N., Kumasaka, T., Yumoto, H., Tanaka, T., Takahashi, S., Takeshita, K., Ohashi, H., Goto, S., Kitamura, H. & Yamamoto, M. (2010). *AIP Conf. Proc.* **1224**, 901–904.
Ikeuchi, M. & Ishizuka, T. (2008). *Photochem. Photobiol. Sci.* **7**, 1159–1167.
Keegan, R. M. & Winn, M. D. (2007). *Acta Cryst.* D**63**, 447–457.
Kikuchi, A., Park, S.-Y., Miyatake, H., Sun, D., Sato, M., Yoshida, T. & Shiro, Y. (2001). *Nature Struct. Biol.* **8**, 221–225.
Kissinger, C. R., Gehlhaar, D. K. & Fogel, D. B. (1999). *Acta Cryst.* D**55**, 484–491.
Maines, M. D., Miralem, T., Lerner-Marmarosh, N., Shen, J. & Gibbs, P. E. (2007). *J. Biol. Chem.* **282**, 8110–8122.
Mantle, T. J. (2002). *Biochem. Soc. Trans.* **30**, 630–633.
Matthews, B. W. (1968). *J. Mol. Biol.* **33**, 491–497.
Miroux, B. & Walker, J. E. (1996). *J. Mol. Biol.* **260**, 289–298.
Otwinowski, Z. & Minor, W. (1997). *Methods Enzymol.* **276**, 307–326.
Salim, M., Brown-Kipphut, B. A. & Maines, M. D. (2001). *J. Biol. Chem.* **276**, 10929–10934.
Schluchter, W. M. & Glazer, A. N. (1997). *J. Biol. Chem.* **272**, 13562–13569.
Sugishima, M., Hagiwara, Y., Zhang, X., Yoshida, T., Migita, C. T. & Fukuyama, K. (2005). *Biochemistry*, **44**, 4257–4266.
Sugishima, M., Migita, C. T., Zhang, X., Yoshida, T. & Fukuyama, K. (2004). *Eur. J. Biochem.* **271**, 4517–4525.
Ueno, G., Kanda, H., Kumasaka, T. & Yamamoto, M. (2005). *J. Synchrotron Rad.* **12**, 380–384.
Vagin, A. & Teplyakov, A. (1997). *J. Appl. Cryst.* **30**, 1022–1025.
Whitby, F. G., Phillips, J. D., Hill, C. P., McCoubrey, W. & Maines, M. D. (2002). *J. Mol. Biol.* **319**, 1199–1210.